Optimal design of slider for stable flying characteristic using 4×1 near-field probe array

Min-su Jung†, Eo-Jin Hong, Kyoung-Su Park*, No-Cheol Park*, Hyun-Seok Yang*, Young-Pil Park*, Sung-Q Lee***, and Kang-Ho Park*****

Key Words : near-field probe array, optical slider, flying ability, flying stability, dynamic characteristics

ABSTRACT

In the information storage development, the trend of the storage device is to increase the recording density. Among such an effort, near-field probe recording is spotlighted as a method of high increasing recording density. For the successfully embodiment of storage device, the actuating mechanism of near-field probe is essentially designed. In this paper, we suggest the slider similar with conventional HDDs and design the slider using near-field probe for the purpose of applying the slider in order to control gap between probe and media. The most important object of slider design is to guarantee the flying ability and stability. For achievement of these design objects, we perform two step of optimal design process. The media is mod! eled as random displacement, which is only considered roughness of disk surface. The design slider is analyzed with dynamic state in assumed media. At this process, the optimal model is confirmed to stable flying stability.

1. Introduction

Recently an improvement of recording density of conventional information storage device nearly comes to its limit, so it has brought up to introduce new storage devices. Among these efforts to next generation storage devices, the near-field probe recording is spotlighted as a method of increasing recording density. For the successfully embodiment of this near-field system, the space between probe and media should be maintained stably. Therefore we propose optical slider in order to stabilize the flying characteristic of probe array. When the mechanism for near-field probe recoding is applied to optical flying slider, the critical problems considered are the low optical throughput and data transfer rate of near-field probe. To increase optical throughput of probe, flying height should be reduced below 20 *nm* [1]. Because of low data transfer rate, the slider should fly in greatly low linear velocity compared to conventional HDDs. Four probes in a row is the possible solution these demerits, however, the difference gap of probes makes error in read/write process. For this reason, roll angle of this slider should be minimized or constrained to reduce the difference of flying height from each probe. Also, when rotary actuator is assumed as a positioning mechanism in this system, differences of skew angle and linear velocity with radial position of disk are occurred. In spite of the greatly low linear velocity and many constraints of operating, flying ability and stability of this slider should be guaranteed for design target. Therefore, an optimal method should satisfy the design target with some constraints. MFD (Method of Feasible Direction), which is optimal method to take precedence of constraints, is employed to maintain constraints. In this paper, optimal design is performed using MFD to guarantee flying ability and stable flying characteristics of slider using near-field probe array. Dynamic characteristics of designed slider are verified by dynamic simulation using random track profile mainly considering roughness.

* *Center for Information Storage Device, Yonsei University*
† E-mail : ballmoon@yonsei.ac.kr
TEL : (02)2123-4677 FAX : (02)365-8460
** Storage System Division, Samsung Electronics Co. Ltd
*** Electronics and Telecommunications Research Institute.

(a) 4x1 near-field probe array (b) Aperture of probe tip

Fig. 1 4x1 near-field probe array

2. Slider for near-field probe array

Different from conventional slider in HDDs, slider for near-field recording has special feature of optical head of probe array and greatly low linear velocity. Slider for near-field probe array should satisfy the static characteristics, such as flying ability in greatly low linear velocity, and minimum roll angle for array probe type. The size of probe tip is about 90 *nm* as shown in Fig. 1. Probe array is located at trailing edge in the membrane (450 μm×250 μm) that becomes an optical path for probe array. The size of slider is compatible with it of nano slider in HDDs. Considering the greatly low recording velocity of optical probe, it is desirable to reduce linear velocity for flying performance of the slider within the limits of the possible. Gram load of slider is decided 2.5 *gf* concerning stability of slider. Diameter of media is 0.85 *inch* and it is small enough for mobile applications. Skew angle varies from -8 to 4.1 *degree* for radius positions of 5.031 *mm* and 9.105 *mm*, respectively.

3. Initial model and its characteristics

The rail shape and distribution of air pressure of initial model are showed in Fig. 2. In this rail shape, air pressure is highly occurred in both sides of slider. As a result, this slider has the strong stability on rolling direction for minimization of difference among flying heights of probe array. Moreover, air pressure should be greatly low in order to protect probe in the membrane for protecting it. In Fig. 2 (a), 4×1 near-field probe array is surrounded with bank structure at the trailing edge and this structure protects near-field probe array against air flow and contamination. In order to determine minimum taking-off velocity of slider, parametric study was performed as to rotational speeds of media in radial positions of ID (5.031 *mm*) and OD (9.105 *mm*).

As a result, slider doesn't take off under 400 *rpm* as shown in Fig. 3. Therefore minimum rotational speed of media is decided on about 430 *rpm* that indicates the linear velocity of 0.41 *m/s* in OD. Flying ability of slider should be guaranteed in such a fairly low linear velocity.

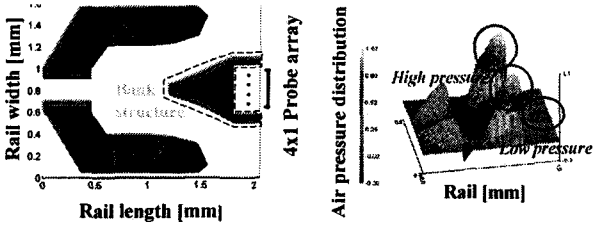

(a) Rail shape (b) Air pressure distribution

Fig. 2 Rail shape and air pressure of initial model

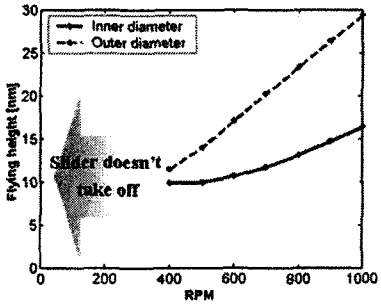

Fig. 3 Taking-off of initial model with rotational speeds

For this reason parametric study was performed in order to seek the factor that is the most sensitive to variation of flying height among many design variables, such as variables related to rail shape, recess height and crown. Fig. 4 shows the results of parametric study of design variables. Through this study, crown is the predominant factor among many design variables for improving flying ability.

4. Optimal design of slider

4.1 Process of optimal design using DOT

Fig. 5 shows the flow chart of optimal design process [2][3]. The assumed design variables apply to objective function and constraints. Their values are evaluated by air bearing simulator. A coefficient of objective function is determined considering non-dimensionless and weighting. The optimal method that directly connects DOT (Design Optimization Tool) with CAE (air bearing simulator) is used to determine the design of slider for near-field probe array. The optimal process is divided into two steps for efficient converges of objective functions. The first optimization is performed to guarantee the flying ability and attitude in static analysis. The object of the second optimization is to improve dynamic flying stability. In the second optimization, flying ability and attitude should be satisfied with design targets. Therefore optimal results of the first optimization should be constraints of the second optimization. For this optimal process, MFD (Method of Feasible Direction)

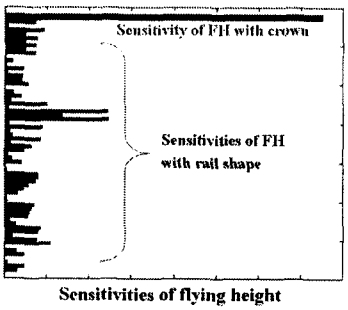

(a) Comparison of sensitivities

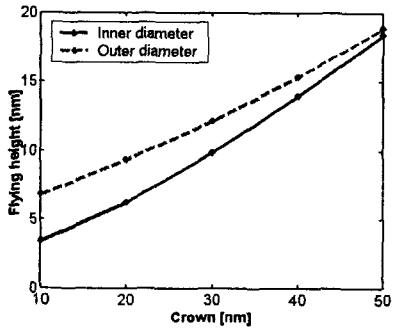

(b) Parameter study with crown

Fig. 4 Crown as predominant factor for flying ability

can be an effective optimal method. This method is a nonlinear programming technique and a fundamental principle of this method is to move from a feasible design to the improved feasible design [4]. The feasible direction and its distance are determined by reducing the cost of objective function within the constraints. Therefore MFD is a suitable optimal method for our design case that needs a strong restriction of many constraints.

4.2 The first optimization

The design target of slider is to keep up flying height of 20 *nm* for high optical throughput of near-field recording using 4×1 probe array. This means guarantee of flying ability in the greatly low linear velocity. Moreover, considering a rotary actuator as a positioning mechanism, flatness of flying height for various radial positions is included in design objects. Objective function and constraints for the first optimization are as follows:

The first optimization

Objective function (*minimize f*)

$$f = \omega_1(probe\,FH_{ID} - 20)^2 + \omega_2(probe\,FH_{OD} - 20)^2 + \omega_3(probe\,FH_{OD} - probe\,FH_{ID})^2 \quad (1)$$

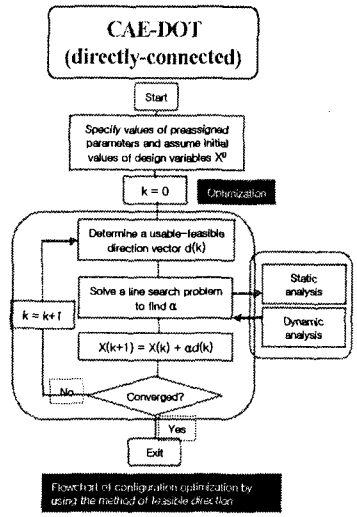

Fig. 5 Design process for optimization

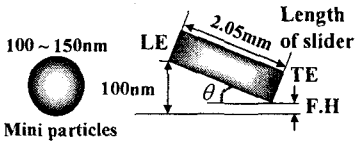

(a) Pitch angle

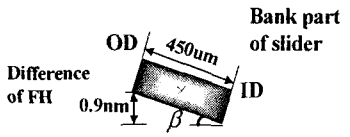

(b) Roll angle

Fig. 6 Constraints with characteristics of 4x1 near-field probe array system

Constraints

$$10\mu rad \le pitch\ angle \le 40\mu rad \quad (2)$$

$$-2\mu rad \le roll\ angle \le 2\mu rad \quad (3)$$

In this optimization, constraints consist of restrictions of pitch and roll angle. Because the size of probe tip is about 90~100 *nm*, the height of leading edge is limited below 100 *nm* to protect probe tip from particles sized bigger than 100 *nm* as shown in Fig. 6 (a) [5]. Pitch angle is restricted in range below 40 μrad that is applicable to the height of 100 *nm* in leading edge for protecting probe array from particles. (Eq. 2) Roll angle relates to the difference of flying height among probes. For that reason, roll angle is restricted within absolute value of 2 μrad that is applicable to the difference of flying height among probes below 1 *nm*. (Fig. 6 (b))

4.3 The second optimization

The second optimization is carried out for improvement of dynamic characteristics with minimization of vertical and pitching sensitivity. Objective function and constraints for the second optimization are as follows:

The second optimization

Objective function (minimize f)

$$f = \omega_1\left(\frac{\Delta FH}{\Delta load}\right)_{OD}^{2} + \omega_2\left(\left(\frac{\Delta load}{\Delta FH}\right)_{OD} - \left(\frac{\Delta load}{\Delta FH}\right)_{ID}\right)^{2} + \omega_3\left(\frac{\Delta pitch\,angle}{\Delta pitching\,moment}\right)_{OD}^{2} + \omega_4\left(\left(\frac{\Delta pitching\,moment}{\Delta pitch\,angle}\right)_{OD} - \left(\frac{\Delta pitching\,moment}{\Delta pitch\,angle}\right)_{ID}\right)^{2} \quad (4)$$

Constraints

$$10\mu rad \le pitch\ angle \le 40\mu rad \quad (5)$$

$$-2\mu rad \le roll\ angle \le 2\mu rad \quad (6)$$

$$19nm \le probe\ FH_{ID}, probe\ FH_{OD} \le 20nm \quad (7)$$

By minimizing objective function, vertical and pitching stiffness is maximized and the difference of vertical and pitching stiffness with radial positions, respectively. (Eq. 4) Constraints of the second optimization cover the results of the first optimization and constraints of pitch and roll angle. (Eq. 5 - 7)

4.4 Optimization results

The optimal model of slider designed by applying two steps optimization process is satisfied with design targets. Table 1 shows the results of the first optimization. The flying height of 20 *nm* is guaranteed and difference of flying height with radial position is reduced below 0.5 *nm*. And pitch and roll angle are in a boundary as shown in Fig. 7. By restriction of roll angle, difference of flying height among probes is limited within 0.5 *nm*. Table 2 shows the results of the second optimization. The vertical and pitching sensitivity are minimized as the results of the second optimization. Therefore vertical and pitching stiffness for dynamic stability are maximized in optimal model. All constraints including flying height in ID and OD are satisfied with limited range as shown in Fig.8. In the first optimization, the increase of crown is the main reason why flying ability is improved in steady state. Accordingly, the crown is increased from 30 nm to 49 nm in the first optimal process. The variations of rail shapes contributed in flatness of flying height in ID and OD. On the other hand, in the second optimization, crown hardly makes a change and rail shapes affected most of improvement of vertical and pitching stiffness.

Table 1 Results of 1st optimization

	Original model	1st optimal model	Improvement (%)
Cost	60.17	0.23	99.6
Ave. FH [*nm*]	12.10	19.79	97.3
ΔFH 1 [*nm*]	2.39	0.23	90.4
ΔFH 2 [*nm*]	0.06	0.48	
Pitch angle [*urad*]	29.39	35.16	Constraints
Roll angle [*urad*]	-0.23	-1.78	

Table 2 Results of 2nd optimization

	1st optimal model	2nd optimal model	Improvement (%)
Cost	107.51	6.33	94.1
Vertical sensitivity [*nm/g*]	6.84	1.31	80.8
Pitching sensitivity [*urad/uN-m*]	4.54	0.46	89.9
Ave. FH [*nm*]	19.79	19.82	
ΔFH 1 [*nm*]	0.23	0.49	
ΔFH 2 [*nm*]	0.48	0.46	Constraints
Pitch angle [*urad*]	35.16	34.42	
Roll angle [*urad*]	-1.78	-1.68	

Δ FH1: FH difference between ID and OD,
Δ FH2: FH difference among probes

Fig. 9 (a) shows the variation of rail shape between initial and final model. With the view of point of air bearing pressure, the highest air pressure is increased than initial model as shown Fig. 9(b).

5. Dynamic simulation

5.1 Disk profile for dynamic simulation

Generally, for higher rotating speeds, the amplitudes of disk topography in the air-bearing frequency range are higher than its lower rotating speeds. Therefore, as rotational speed of disk decreases, the surface wavelength linearly decreases to low frequency [6].

In this paper, rotating speed of slider for near-field probe array is greatly low, and frequencies of high wavelengths of large amplitude (runout, waviness, and flutter) become greatly low. Difference between frequencies of high wavelengths and natural frequency of air-bearing is so wide that dynamic characteristics aren't greatly influenced by these wavelengths. For that reason, low wavelengths with low amplitude (roughness) deserves much consideration for evaluation of dynamic characteristics.

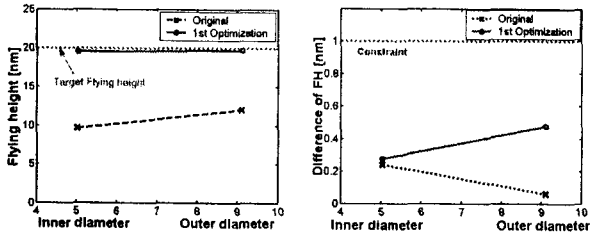

(a) Flying height (b) Difference of FH among probes

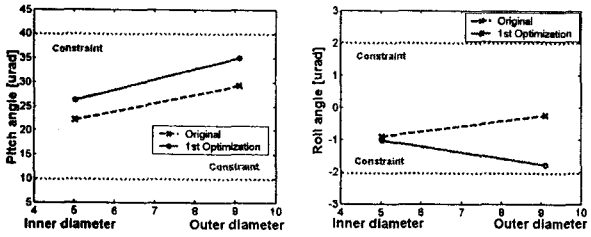

(c) Pitch angle (d) Roll angle

Fig. 7 Results of 1st optimization

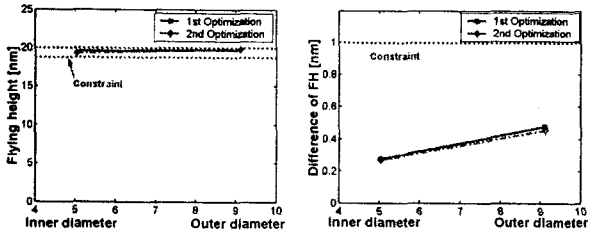

(a) Flying height (b) Difference of FH among probes

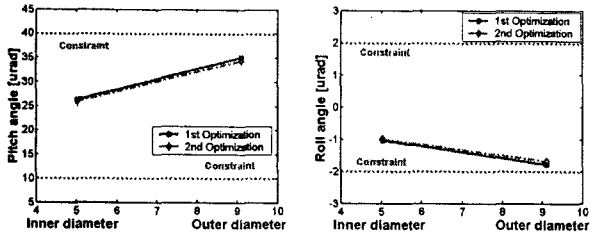

(c) Pitch angle (d) Roll angle

Fig. 8 Results of 2nd optimization

Random disk profile considering roughness of disk is mainly generated by modified midpoint displacement method [7]. This method is to expend random disk profile from lower frequency profile to higher frequency. In this paper, fundamental period and number of additional frequency are 16 μs and 5 times, respectively. The relationship between variances of previous and additional random profile equals to the form of Eq. (7)

$$\sigma^2_{n+1} = \left(\frac{1}{2}\right)^p \sigma^2_n \qquad (7)$$

(p; scaling parameter)

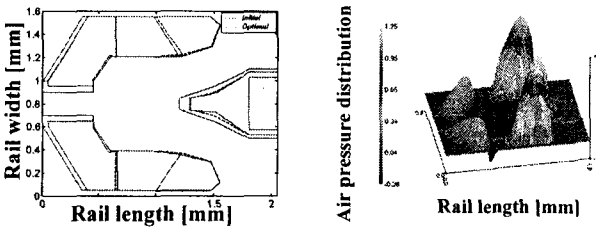

(a) Rail shape (b) Air pressure distribution

Fig. 9 Rail shape and air pressure of optimal model

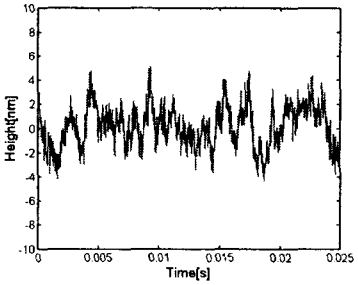

Fig. 10 Generated random disk profile

'p' value determines the characteristics of amplitude with power spectrum of the disk profile. When the 'p' value is increased, amplitudes of high frequency components are decreased. We generate random disk profile as 'p' value = 1. The Fig. 10 shows the generated random disk profile that has the standard deviation of 2.0 *nm*, the maximum height of 5.13 *nm* and frequency range of 62.5 *kHz* ~ 2 *MHz*. Also, preload of used suspension for dynamic simulation is 2.5 *gf* and vertical, pitching and rolling stiffness are 36.37 *N/m*, 0.0799 *N-m/rad* and 0.428 *N-m/rad*, respectively.

5.2 Results of dynamic simulations

Table 3 and Table 4 show the results of dynamic simulation with both original and optimal model. Average flying height, pitch angle and roll angle according to results of dynamic simulation nearly agree with results of static analysis. In optimal model, roll angle increases to 2.3 μrad that are satisfied with constraints. And difference of flying height among probes for the roll angle of 2.3 μrad is within the design target of 1 *nm*. Table 4 shows the variations of dynamic characteristics with optimization. The standard deviations of flying height and roll angle are improved but those of pitch angle and air bearing force are deteriorated as shown in table 4. Because crown is increased to guarantee the flying ability in the first optimization, dynamic instability is increased and the standard deviations of the pitch angle and the air bearing force are deteriorated. As shown in Fig. 11 and Fig. 12, considering vertical direction, standard deviation of flying height is decreased to 9.6% in spite of increasing

Table 3 Comparison of dynamic characteristics between original and optimal model

Standard deviation	Original model	Optimal model	Improvement (%)
Flying height [nm]	1.15	1.04	+9.6
Pitch angle [urad]	1.37	1.55	-13.1
Roll angle [urad]	0.29	0.15	+48.3
Air bearing force [gf]	0.0515	0.0697	-35.3

of variance of air bearing force. Therefore we can say that the dynamic stability of optimal model to maintain flying height is improved. This has the reason that the dynamic characteristics are improved by the second optimization. The increased crown has a high effect on instability in pitching direction. Therefore the standard deviation of pitch angle in optimal model is increased despite improvement of pitching sensitivity by the second optimization.

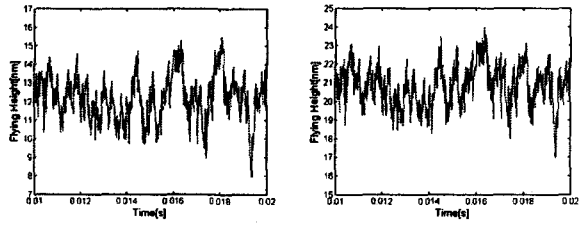

(a) Original model (b) Optimal model

Fig. 11 Comparison between original and optimal model for variation of flying height

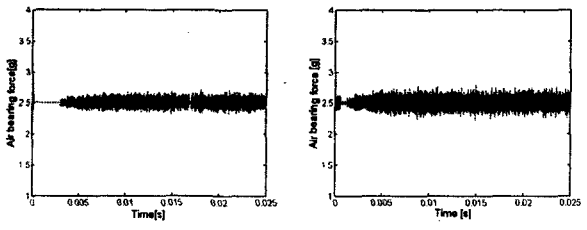

(a) Original model (b) Optimal model

Fig. 12 Comparison between original and optimal model for variation of air bearing force

6. Conclusions

We designed the slider for 4x1 near-field probe array in order to guarantee flying ability and stability. For design of this slider, two steps of optimal process were performed by directly connected method using DOT of MFD algorithm. As a result, flying ability was guaranteed in greatly low linear velocity by the first optimization and vertical and pitching stiffness were improved by the second optimization. Moreover, all constraints related to specifications of near field probe array system were satisfied with the feasible region. For guarantee of flying ability, crown of slider was the most effect design parameter in the first optimization but the increasing of crown for flying ability increased instability of slider. In the results of dynamic simulation by random disk profile, flying height modulation was improved in optimal model in spite of increasing instability of slider. Therefore, we can say that dynamic stability to maintain flying height was improved in optimal model by the second optimization.

Acknowledgement

This work was funded by the Korea Science and Engineering Foundation (KOSEF) through the Center for Information Storage Device (CISD) Grant No. R11-1997-042-11001-0.

References

(1) K. B. Song, E. K. Kim, S. Q. Lee and K. H. Park (2003), "Fabrication of a High-Throughput Cantilever-Style Aperture tip by the Use of the Bird's-Beak Effect ", *Jpn. J. Appl. Phys*, Vol. 42. pp. 4353-4356.

(2) T. S. Kang, D. H. Choi and T. G. Jeong (2001), "Optimal Design of HDD Air-Lubricated Slider Bearings for Improving Dynamic Characteristics and Operating Performance", *ASME J. of Tribol.*, Vol. 132. pp. 541-547.

(3) H. Hashimoto and Y. Hattori (2000), "Improvement of the Static and Dynamic Characteristics of Magnetic Head Sliders by Optimum Design", *ASME J. of Tribol.*, Vol. 122, pp. 280-287.

(4) G. Zoutendijk (1960), "Methods of Feasible Directions", *Elsevier*, Amsterdam.

(5) J. Li, B. Liu, Y. Ma, W. Hua and T. C. Chong (2001), "ABS Design for Anti-Surface Borne Particles", *IEEE Trans. Mag.*, Vol. 37, pp 1802-1805.

(6) Q. H. Zeng, B. H. Thornton, D. B. Bogy and C. S. Bhatia (2001), "Flyability and Flying Height Modulation Measurement of Slider with Sub-10 nm Flying Heights", *IEEE Trans. Mag.*, Vol. 37, pp. 894-899.

(7) K. Ono, K. Takahashi and K. lida (1999), "Computer Analysis of Bouncing Vibration and Tracking Characteristics of a Point Contact Slider Model Over Random Disk Surfaces", *ASME J. of Tribol.*, Vol. 121, pp 587-595